PUBLICATION V

# Probabilistic simulation of cable performance and water based protection in cable tunnel fires

In: Nuclear Engineering and Design,
Vol. 241, No. 12, pp. 5263–5274.

Nuclear Engineering and Design 241 (2011) 5263–5274

Contents lists available at SciVerse ScienceDirect

Nuclear Engineering and Design

journal homepage: www.elsevier.com/locate/nucengdes

# Probabilistic simulation of cable performance and water based protection in cable tunnel fires

Anna Matala*, Simo Hostikka

*VTT, P.O. Box 1000, FI-02044 VTT, Finland*

ARTICLE INFO

*Article history:*
Received 19 January 2011
Received in revised form 29 August 2011
Accepted 11 September 2011

ABSTRACT

Nuclear power plants contain a significant amount of fire load in form of electrical cables. The performance of the cables is interesting both from the fire development and system failure viewpoints. In this work, cable tunnel fires are studied using numerical simulations, focusing on the fire spreading along power cables and the efficiency of the water suppression in preventing the cable failures. Probabilistic simulations are performed using Monte Carlo technique and the Fire Dynamics Simulator (FDS) as the deterministic fire model. The primary fire load, i.e. the power cables are modelled using the one-dimensional pyrolysis model, for which the material parameters are estimated from the experimental data. Two different water suppression systems are studied. The simulation results indicate that using either suppression system decreased the heat release rate in the tunnel to less than 10% of the non-suppressed case. Without water suppression, the cables of the second sub-system were damaged in almost all fires, but when either of the studied water suppression systems was used, the probability of the cable failures was decreased to less than 1%. This result indicates that in current scenario, the probability of losing both sub-systems is determined directly by the suppression system unavailability.



## 1. Introduction

The safety of nuclear power plants relies heavily on concepts such as defence-in-depth and redundancy. For fire safety, the defence-in-depth means that attempts are made both to prevent the ignition of fires and to prepare for their consequences. Fire may also challenge the redundancy if it can penetrate through the barriers between the redundant parts. Sometimes the components of two subsystems can be located in the same room. This can challenge the safety of the plant especially when dealing with cables placed in the cable spreading rooms and cable tunnels. If the cables belonging to the other subsystem catch fire, they can be assumed to have already failed electrically. From the viewpoint of Probabilistic Risk Assessment (PRA), the probability of the failure in the other subsystem is extremely interesting (Paté-Cronell and Dillon, 2006) and several different methods have been used for the computation of the failure probability. One of the methods is based on the use of a severity factor which is the likelihood of those heat release rates for a given fire source that can cause a failure of a given target. As mentioned in the guidance document by the U.S. Nuclear Regulatory Commission (NRC, 2005), the application of severity factors has been a point of debate in past PRA approaches because fire severity-likelihood relationships are heavily influenced by expert judgment. Additional difficulty comes from the fact that neither the fire sources nor the targets may be explicitly specified in spaces such as cable tunnels because both of them can exist anywhere in the space.

The risk of losing both subsystems can be reduced by several means, such as physical separation between the subsystems, choice of cable materials and the use of fire suppression systems. The requirement for the physical separation is typically 6.2 m (20 ft), as suggested by the U.S. NRC in 10 CFR 50.48 (Appendix A and R). If the minimum distance cannot be fulfilled, some barriers should be placed between the cable trays. In some installations, information and control (IC) cables are placed inside metal cable conduits, which act also as thermal barriers. The sufficiency of the 6.2 m separation distance between the polyvinyl chloride (PVC) cable trays was studied by Shen (2006) using Fire Dynamic Simulator (FDS) simulations. In this work, the separation distance is fixed according to the actual case from a Finnish nuclear power plant (NPP), and the focus is in the simulation of fire spreading and fire suppression.

The cable materials are a versatile group of different kinds of plastics. Although modern, flame-retardant and non-corrosive cable sheath materials are on the market, the cables of the existing

*Abbreviations:* CFD, Computational Fluid Dynamics; DSC, Differential Scanning Calorimetry; FDS, Fire Dynamics Simulator; GA, Genetic Algorithm; HCl, hydrochloric acid; HRR, heat release rate; IC, information and control (cable); LHC, Latin Hypercube (sampling); MC, Monte Carlo (simulation); MLR, mass loss rate; NPP, nuclear power plant; PFS, Probabilistic Fire Simulator; PMMA, polymethyl methacrylate; PRA, Probabilistic Risk Assessment; PVC, polyvinyl chloride; RTI, response time index; TGA, Thermogravimetric Analysis.

* Corresponding author. Tel.: +358 405152535.
*E-mail address:* anna.matala@vtt.fi (A. Matala).

0029-5493/$ – see front matter © 2011 Elsevier B.V. All rights reserved.
doi:10.1016/j.nucengdes.2011.09.014

**Nomenclature**

| | |
|---|---|
| $A$ | pre-exponential factor ($s^{-1}$) |
| $c_p$ | specific heat capacity (kJ/(kg K)) |
| $C$ | $C$-factor of sprinkler |
| $E$ | activation energy (kJ/mol) |
| $d$ | thickness (m) |
| $\Delta H$ | heat of reaction (kJ/kg) |
| $\Delta H_c$ | heat of combustion (MJ/kg) |
| $k$ | thermal heat conductivity (W/(m K)) |
| $L$ | length characteristic of the smoke detector geometry |
| $N$ | reaction order |
| $q'''$ | source term in heat conductive equations |
| $Q_{max}$ | maximum heat release rate of the initial burner (kW) |
| $R$ | universal gas constant, 8.314510 J/(mol K) |
| RTI | RTI value of the sprinkler detector ($(ms)^{1/2}$) |
| $T_a$ | activation temperature of the sprinkler detector (°C) |
| $t_{peak}$ | time of the maximum heat release rate of the burner (s) |
| $u$ | the free stream velocity (in sprinkler and smoke detector) |
| $x$ | co-ordinate along the tunnel (m) |
| $y$ | horizontal co-ordinate across the tunnel. Residue yield (kg/kg) |
| $Y_c$ | mass fraction of smoke in the sensing chamber of the detector |
| $Y_e$ | Mass fraction in the external free stream (of smoke detector) |
| $z$ | vertical co-ordinate (m) |
| $x_b$, $z_b$ | horizontal and vertical co-ordinates of the initial burner |

*Greek letters*

| | |
|---|---|
| $\beta$ | volume fraction of water in the gas stream |
| $\rho$ | density ($kg/m^3$) |
| $\sigma$ | Stefan–Boltzmann constant, $5.67051 \times 10^{-8}$ W/($m^2K^4$) |

power plants are often made of conventional plastics, such as PVC. Loss of the hydrochloride acid (HCl) gas from heated PVC acts as "in-built" flame-retardant, thus reducing the burning rate as compared to many other non-flame retardant polymers. However, burning PVC produces lots of smoke and toxic gases. Quite recently, Ferng and Liu (2011) used the FDS code to investigate the burning characteristics of the electrical cables in cone calorimeter experiments. In their article, they compared several gas phase measurements of cable and polymethyl methacrylate (PMMA) samples, but did not report how the cables were described in the simulations. In this work, the thermal decomposition of PVC cables is modelled using the pyrolysis model of the FDS code. The model parameters are estimated from small scale experiments (Matala et al., 2008). The occurrence of electrical failures in the target subsystem is predicted using temperature criteria, as demonstrated by Andersson and Van Hees (2005). This method was recently validated in Dreisbach and McGrattan (2008) and Dreisbach et al. (2010).

The suppression systems may be designed either to suppress the fire or to protect the subsystems from each other, or both. In fire-PRA, it is important to consider that the reliability of the active systems is not perfect. The sprinkler system, for instance, may suffer from system or component failures. The water suppression system of the room may fail to activate or problems may appear in individual nozzles or valves. The efficiency of the system also depends on the details of the design, such as nozzle placement, nozzle characteristics, sensitivity of the activating components or water flow rate. Chien et al. (2006) used FDS to study the effects of shielding and sprinkler spacing and pressure on the fire development in a NPP cable room.

In this work, we propose a probabilistic method of numerical simulation that gives the conditional probability of second subsystem failure, in case of *any* ignition in the cables of the tunnel. Monte Carlo (MC) simulations are performed using Probabilistic Fire Simulator – PFS (Hostikka and Keski-Rahkonen, 2003) for the statistical operations and FDS (McGrattan et al., 2007, 2010) as the deterministic fire model. The most important boundary conditions of the fire simulations are treated as random variables and the deterministic simulations are repeated many times with different input parameters. The statistical distributions of the random variables are based on the geometrical properties of the cable tunnel under consideration or expert opinions. The work demonstrates how the state-of-the-art deterministic fire simulation can be used in the probabilistic framework. The goals of the work are

1. to evaluate the effectiveness of two different water based suppression systems in the protection of the second subsystem in case of power cable fire,
2. to find out the probabilities of cable failures in cases when the suppression system does or does not operate, and
3. to evaluate the conditions affecting the operation of fire fighters.

The numerical tools used in this work are shortly described in Section 2. The details of the cable tunnel under consideration and its features, including the fire source, suppression system and the fire detection are described in Section 3. This section also describes how these aspects are implemented as boundary conditions for numerical simulations. The selection of random variables is described in Section 4 and the results of the probabilistic simulations in Section 5. The conclusions are presented in Section 6.

## 2. Overview of the numerical methods

### 2.1. Fire Dynamics Simulator (FDS)

FDS is developed as a co-operation between NIST (National Institute of Standards and Technology) and VTT Technical Research Centre of Finland. It models fire-driven flows by solving numerically a low-Mach number form of the Navier–Stokes equations. The time dependent field of thermal radiation is solved using Finite Volume Method for radiation accompanied by the gray gas model for the gas phase emission, absorption and scattering. The governing equations are explained in detail in the Technical Reference Guide of FDS (McGrattan et al., 2007). Here we only provide a brief summary of the models used for computing the specific features of the simulation.

In the current simulations, the fire development is predicted by the code itself – not prescribed by the user. In terms of Computational Fluid Dynamics (CFD) boundary conditions, this means that the inflow rate of fuel gas at cable surfaces is computed using a pyrolysis model. The heat conduction inside the solid materials is solved using the one-dimensional heat conduction equation

$$\rho_s c_s \frac{\partial T_s}{\partial t} = \frac{\partial}{\partial x} k_s \frac{\partial T_s}{\partial x} + q_s''', \quad (1)$$

where $x$ is the internal distance from the material surface, $T_s(x,t)$ is the solid phase temperature and $\rho_s$, $c_s$ and $k_s$ are material properties. Source term $q_s^m$ consists of heats of reaction due to the thermal decomposition reactions. Each solid surface can consist of multiple layers, and each can consist of a mixture of multiple material

components. Each of the components can undergo several reactions yielding solid residue or gaseous products, such as fuel for the gas phase combustion. The reaction rates are calculated using Arrhenius equation

$$\frac{\partial}{\partial t}\left(\frac{\rho_i(x,t)}{\rho_0}\right) = A\left(\frac{\rho_i(x,t)}{\rho_0}\right)^N \exp\left(-\frac{E}{RT_s(x,t)}\right), \quad (2)$$

where $A$ is the pre-exponential factor, $E$ is the activation energy, $N$ is the reaction order and $R$ is the universal gas constant. $\rho_i$ is the mass concentration of the $i$th solid phase species and $\rho_0$ is the initial density of the layer.

The coefficients in Eqs. (1) and (2) are not well known constants that would be listed in handbooks. Instead, they must be estimated from experimental data. In this work, the experimental methods used were Thermogravimetric Analysis (TGA) along with Differential Scanning Calorimetry (DSC) and cone calorimeter. In the beginning of the estimation process, the reaction paths were determined from qualitative analysis of TGA and DSC results. The kinetic parameters $A$, $E$ and $N$ were then estimated from the TGA data. The remaining unknown parameters were estimated from the cone calorimeter data, which was obtained both for each of the major cable components separately and for the complete cable. This stage involves modelling of the cone calorimeter experiment and making the most important pyrolysis model approximations concerning the representation of real cables as one-dimensional objects.

Each degradation reaction requires the total of eight unknown parameters ($A$, $E$, $N$, $y$, $k_s$, $c_s$, $\Delta H$, $\Delta H_c$). As there are several components in each cable and each component may degrade with multiple degradation steps, the number of estimates and therefore the complexity of the estimation task increase rapidly. Furthermore, the target equations are strongly non-linear with local minima which make the traditional, gradient-based optimization methods inefficient in finding the best combination of model parameters. For these reasons, the parameter estimation was mainly done using Genetic Algorithm (GA) (Matala et al., 2008), which has proved to be an effective tool for the parameter estimation for fire engineering needs. GA is based on the idea of evolution or the survival of the fittest. A group of randomly chosen candidate solution converges towards a local optimum during the iteration steps. The operations are stochastic and the probabilities are based on the fitness of the model. In this work, the number of individuals of each four subpopulation was 20 making altogether 80 candidate solutions. The iterations were manually interrupted after necessary convergence was achieved, typically after 100–200 generations. The other parameter values used for GA in this work are more profoundly listed in paper of Matala et al. (2008). Thermal parameters can be also estimated manually using predetermined information concerning the effects of the various parameters on the cone calorimeter result. For example, high thermal conductivity is known to produce longer ignition times. This method can be used instead of the numerically expensive GA or to supplement it.

When estimating parameters from the experimental data, it is important to understand the approximations and limitations of the model. The cone calorimeter model used here approximates the cable geometry as a rectangular slab with homogenous layers. The assessment of the pyrolysis model validity should be based on the accuracy of predicted time to ignition and time evolution of three quantities: heat release rate, mass loss rate and effective heat of combustion.

Automatic sprinklers are activated when the temperature of the sensing element of the device $T_l$ exceeds the predetermined activation temperature. The heat conducted away from the element by the mount is not taken into account. The temperature is estimated from the differential equation

$$\frac{dT_1}{dt} = \frac{\sqrt{|u|}}{\mathrm{RTI}}(T_g - T_l) - \frac{C_2}{\mathrm{RTI}}\beta|u|, \quad (3)$$

where $T_g$ is the gas temperature, $u$ is the stream velocity and $\beta$ is the volume fraction of liquid water in the gas stream. Response time index (RTI) defines the sensitivity of the detector and $C_2$ is constant $6 \times 10^6$ K/(m/s)$^{1/2}$.

The transport of liquid water is computed using a Lagrangian method, where the water spray consists of a sampled set of spherical droplets. For each type of sprinkler head/nozzle, the user defines the median droplet diameter $d_m$, droplet speed and angular direction where the droplets are inserted. The droplet size distribution consists of a combination of Rosin–Rammler and log-normal distributions, and is expressed with Cumulative Volume Fraction

$$F(d) = \begin{cases} \dfrac{1}{\sqrt{2\pi}} \displaystyle\int_0^d \frac{1}{\sigma d'} \exp\left(-\frac{|\ln(d'/d_m)|^2}{2\sigma^2}\right) dd', & d \le d_m \\ 1 - \exp\left(-0.693\left(\dfrac{d}{d_m}\right)^{\gamma}\right), & d_m < d \end{cases}, \quad (4)$$

where empirical constants are $\sigma = 0.6$ and $\gamma = 2.4$. The variation in pipe pressure $P$ due to the opened sprinkler heads/nozzles affects the droplet boundary conditions: flow rate and droplet speed are proportional to $P^{1/2}$, and the median diameter to $P^{-1/3}$.

### 2.2. Probabilistic Fire Simulator

The MC simulations were carried out using PFS – tool that has been developed at VTT. In addition to the actual Monte Carlo simulations, PFS can be used as an interface for several fire models, including FDS (Hostikka and Keski-Rahkonen, 2003; Hostikka, 2008). PFS can handle all three phases in the MC simulations: sampling, simulation and results post-processing. The user interface is an excel spreadsheet that uses macros. In the interface, there is an individual sheet dedicated for each operation, and user can easily apply it to match the requirements of each task. In this work the sampling is done using Latin Hypercube (LHC), which reduces the necessary sample size compared to traditional Monte Carlo sampling (McKay et al., 1979; Stein, 1987). PFS creates the necessary input for FDS simulations using the previously created random values and user-defined template. After that, PFS performs the FDS simulations for all the input files separately. For more efficiency and parallel processing, this part can also be done separately from the earlier phase. In the post-processing phase the program reads the outputs from all simulations and performs the statistical analysis comparing the input variables and output values.

## 3. Fire scenario and modelling

### 3.1. Cable tunnel

The dimensions of the simulated tunnel are 95 m × 2.8 m × 5.5 m (height). The room has IC and power cables from two independent subsystems physically separated by a 1.3 m wide corridor. The cables are placed along the long sides of the tunnel, one subsystem at each side. The subsystems have 10 trays of IC cables in the bottom and 5 trays of power cables on the top, as illustrated in Fig. 1. The tunnel walls are made of 30 cm concrete. The properties of concrete (thermal conductivity, specific heat capacity and density) are treated as random variables to consider the uncertainty associated with their numeric values.

For the computations the tunnel was divided into three CFD meshes. The first mesh is the most important one and contains the cable trays and sprinkler heads. It is 15 m long and discretized with

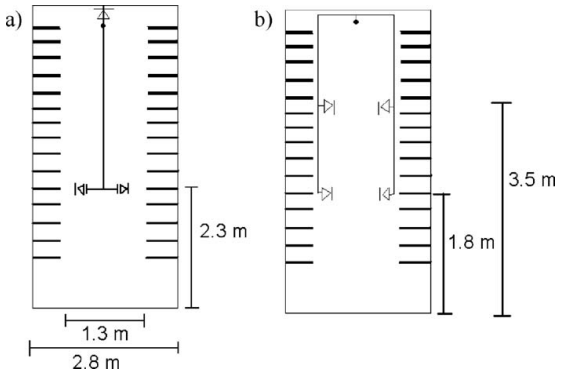


**Fig. 1.** Cross-section of the cable tunnel and the sprinkler nozzles of System 1 (a) and System 2 (b).

10 cm grid cells. It is assumed to be large enough to reveal all the relevant dynamics of the fire, cable failures and suppression system. The spatial resolution is coarse when considering the geometrical length scales of the flames between the cable trays, but sufficiently fine to capture the main characteristics of the fire spreading, provided the igniting fire source is large enough. The two remaining meshes are necessary just for the correct amount of available air. They have coarser grid size and no cable trays or sprinklers to speed up the simulations. The lengths of these meshes are 5 m and 75 m, and computational resolutions 0.30 m and 0.60 m, respectively.

### 3.2. Electrical cables

#### 3.2.1. Power cables

Numerical simulation of fire spreading on cable trays is the most challenging part of the fire simulations and practically unvalidated class of FDS applications. Due to the involvement of a wide range of different physical scales, it is extremely difficult to numerically predict the development of the fire from small ignition. Our philosophy of modelling the spreading cable fire was to prescribe the initial fire up to the size where the fire can be resolved by the CFD mesh used for the tunnel scale simulation and realistic predictions of the thermal environment can be expected. Beyond that point, the development of the fire is predicted by the cable pyrolysis model.

The initial source of the fire in these simulations is a local fire on one of the power cable trays. The fire starts from a small local ignition and develops to a scale that corresponds to a roughly 2-m long section of 3 trays of PVC cables. It is prescribed as a burner with heat release rate curve following roughly an experimental result from a horizontal cable fire test (Mangs and Keski-Rahkonen, 1997). The approximation of the experimental curve is shown in Fig. 2. To account for the geometrical and material related variations between the experiment and the target tunnel, and the uncertainty concerning the actual ignition mechanism, some randomness is added by setting the peak heat release rate and the time of the peak as triangularly distributed random variables. The details and exact values are discussed in Section 4. Other times and the shape of the curve are kept similar to the experimental curve. The fire starts always from the same subsystem. The burner size is $0.75 \times 0.75\ \mathrm{m}^2$ and its $x$- and $z$-location are random variables.

It is important to notice that the initial fire source is not coupled with the activation of the suppression systems. The model is therefore likely to underestimate the efficiency of the sprinklers.

Each of the power cable trays is assumed to contain one layer of power cables. In reality the cable tunnels contain many different types of cables but in the simulations they are approximated using

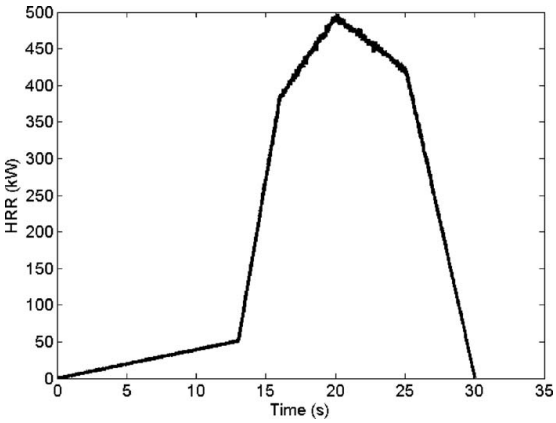


**Fig. 2.** Approximation of the experimental power cable heat release rate.

a numerical model of NOKIA AHXCMK 10 kV $3 \times 95/70\ \mathrm{mm}^2$ power cable (Fig. 3). The cable components and their properties in the original cable are listed in Table 1.

The reaction paths and kinetic parameters of the degradable components (sheath, insulation and filler) were estimated from separate TGA results. The reaction paths used for the components are shown below

$$\begin{aligned} \text{Sheath} &= \begin{cases} \text{volatile component}\,(56\%) \\ \text{solid}\,1\,(11\%) \rightarrow \text{char} + \text{fuel gas} \\ \text{solid}\,2\,(33\%) \rightarrow \text{char} + \text{fuel gas} \end{cases} . \\ \text{Insulation} &= \text{solid} \rightarrow \text{char} + \text{fuel gas} \\ \text{Filler} &= \text{solid} \rightarrow \text{char} + \text{fuel gas} \end{aligned} \tag{5}$$

A comparison between the experimental and simulated TGA results in Fig. 4a shows that the model can predict the TGA curves very accurately. The simplification of replacing hundreds of chemical reactions just by few is very strong but necessary considering the complexity of the whole simulation problem. It is desirable to have a model that tries to reproduce the main characteristic behaviour of the degrading cable in a computationally affordable way, requiring as few parameters as possible.

The thermal parameters were estimated from the cone calorimeter experiments that were performed separately for each of the components (sheath, filler rods and insulation with conductor), considering three different quantities: heat release rate, mass loss rate and effective heat of combustion. A comparison of the measured and predicted heat release rates for the components are shown in Fig. 4b. Thermal and kinetic model parameters are listed in Table 2. Finally, the geometrical parameters of the 1D-approximation were estimated using the data of the complete cable, shown in Fig. 4c. The 1D model of the cable consists of four layers:

1. sheath 2.5 mm,

**Table 1**
Components and mass fractions of the NOKIA AHXCMK 10 kV $3 \times 95/70\ \mathrm{mm}^2$ cable.

| Component | Mass fraction (kg/kg) | Linear mass (g/m) | Thickness (mm) |
|---|---|---|---|
| Sheath (PVC) | 0.228 | 600 | 2.5 |
| Copper binding | 0.15 | 400 | – |
| Filler rods | 0.08 | 210 | 10 |
| Insulator (PEX) | 0.25 | 650 | 3 |
| Conductor | 0.27 | 710 | 15 |
| Plastics and crepe paper | 0.022 | 58 | – |

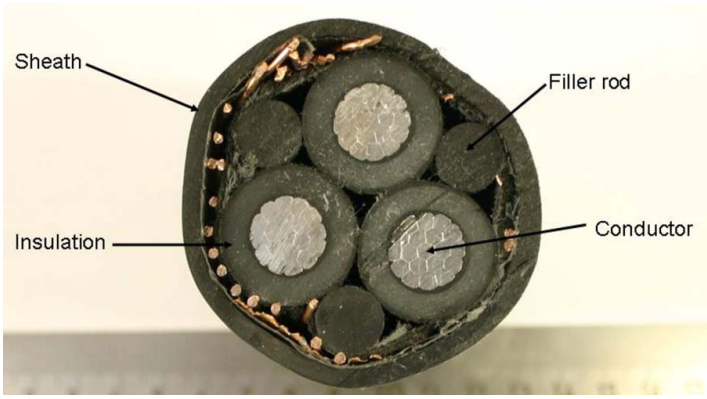


**Fig. 3.** Cross-section of the NOKIA AHXCMK 10 kV 3 × 95/70 mm² power cable.

2. insulation and filler 12 mm,
3. sheath 5.0 mm,
4. metal 8.234 mm.

When the model created in cone calorimeter was applied to the cable tunnel simulations, the 1D pyrolysis model was associated with both top and bottom surfaces of the obstacles representing the cable trays. As the same material point was allowed to burn from two sides of the obstacles, the layer thicknesses were divided by two to ensure the conservation of combustible mass.

The gas phase combustion reaction is specified as

$$C_2H_3Cl + 2.75O_2 \rightarrow 2CO_2 + 1.5H_2O + Cl + 5\%\,\text{soot} + 40\,\text{MJ/kg heat} \quad (6)$$

where the product chlorine acts as a simple non-reacting species, while in reality, the chlorine appears as HCl.

### 3.2.2. IC cables

IC cables are a versatile group of electrical cables. They are located inside of a cable conduit in the 10 lowest cable trays at both sides of the corridor. The conduits are made of steel sheets, 1 mm thick at the bottom and 2 mm on the sides and top. Because of the cable conduit, the IC cables do not contribute to the fire. However, the heating of the cables inside the conduit is computed for the prediction of cable failures. The IC cables are simulated with a 1D heat transfer solver as a layer of non-reacting PVC covered by a layer of steel. The thermal properties for non-reacting PVC were $k_s = 0.16\,\text{W/(m K)}$, $c_s = 1.05\,\text{kJ/(kg K)}$ and $\rho_s = 1400\,\text{kg/m}^3$. The cable failures are assumed to take place when the temperature at the depth corresponding to electrical insulation layer reaches a pre-defined critical temperature. The method is essentially the same as proposed by Andersson and Van Hees (2005) and further developed by U.S. NRC in Dreisbach and McGrattan (2008), but makes use of the thermal properties of the specific cables in the current scenario. In the works of Andersson and Van Hees and U.S. NRC, the thermoplastic cables, such as PVC cables, were found to have a critical temperature around 200 °C. In this work, two different failure criteria, 180 °C and 220 °C, were used in order to study the sensitivity of the failure probability. The cable temperatures were monitored in all locations of the tunnel, and the highest observed temperature was compared against the chosen failure criteria.

### 3.3. Suppression systems

Two different water suppression systems were studied. Both systems consist of a control valve and open nozzles. The control valves are located in the middle of the corridor, 10 cm below the ceiling and 3.5 m from each other in *x*-direction, as illustrated in Fig. 1. The control valve detects the temperature under the ceiling and discharges the water to the open nozzles below. In the model, the suppression system was only included to the first mesh. To the length of the first mesh it means four independently operating units.

The spray nozzles were characterized for the model using simple experiments. The flow rates at known pressure were first measured to determine the nozzle *K*-factors. The water distributions of the nozzles were then measured by covering the floor by empty pans and spraying the water through the nozzle at known water pressure. After pre-determined time, the amount of the water in the pans was measured and the water distribution as a function of horizontal distance from the nozzle was determined. The model parameters (spray angle, droplet velocity, droplet insertion offset and droplet median diameter) were estimated from the experimental results where the nozzle was in pendent position. The model was then validated using the results of a horizontally positioned nozzle. The RTI value and sprinkler activation temperature are variables in the MC simulations.

**Table 2**
Model parameters for the NOKIA AHXCMK 10 kV 3 × 95/70 mm² cable.

| Material | Layer | $\rho$ | $A$ | $E$ | $n$ | $y$ | $k_s$ | $c_s$ | $\Delta H$ | $\Delta H_c$ |
|---|---|---|---|---|---|---|---|---|---|---|
| Sheath 1 (56%) | 1, 3 | 1501 | $1.78 \times 10^9$ | 127 | 1 | 0 | 0.1 | 2.5 | 200 | – |
| Sheath 2 (11%) | 1, 3 | 1501 | $8.64 \times 10^{12}$ | 290 | 1 | 0.474 | 0.05 | 1.0 | 300 | 20 |
| Sheath 3 (33%) | 1, 3 | 1501 | $6.61 \times 10^8$ | 159 | 1 | 0.618 | 0.05 | 1.0 | 1700 | 50 |
| Insulation | 2 | 1039 | $6.53 \times 10^{12}$ | 218 | 0.308 | 0 | 0.2 | 3.5 | 2500 | 35 |
| Filler | 2 | 950 | $6.27 \times 10^{12}$ | 220 | 0.135 | 0 | 0.15 | 3.0 | 2000 | 35 |
| Metal | 4 | 3042 | – | – | – | – | 10.0 | 8.5 | – | – |
| Char | 1, 3 | 385 | – | – | – | – | 0.4 | 1.5 | – | – |

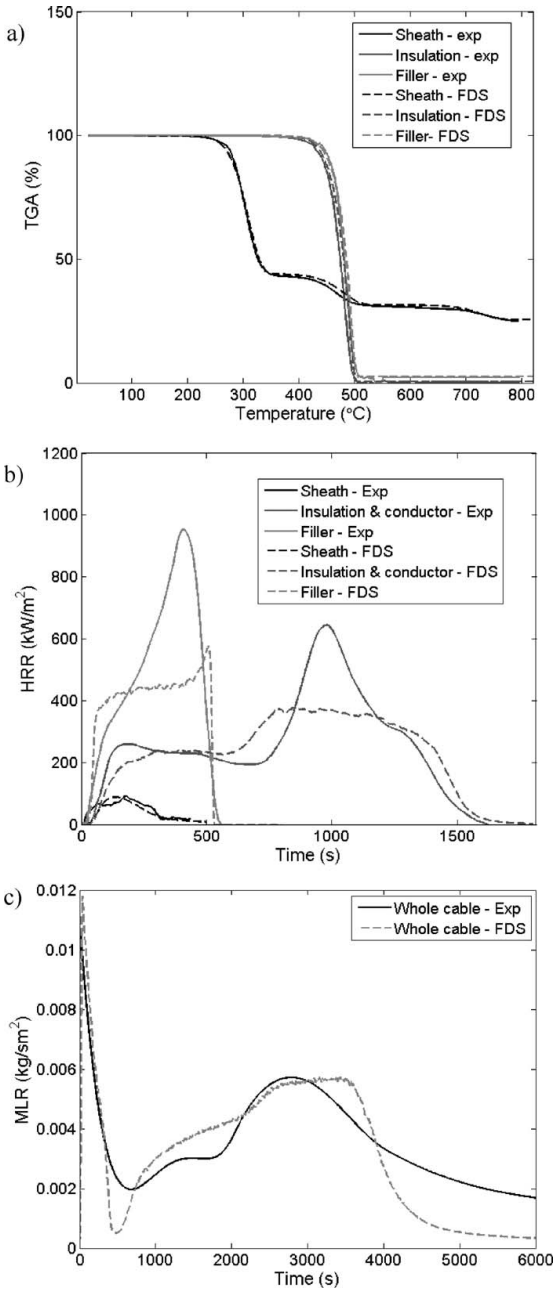


**Fig. 4.** Comparison of the experimental and simulated results. (a) TGA in nitrogen at heating rate 10 K/min. (b) Heat release rate of the components from cone calorimeter at 50 kW/m$^2$ heat flux. (c) Mass loss rate of the whole cable from cone calorimeter at 50 kW/m$^2$ heat flux.

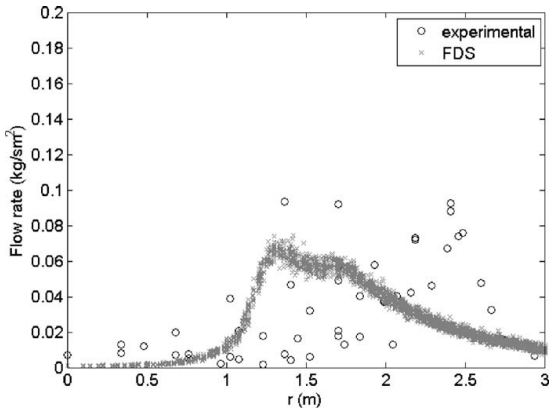


**Fig. 5.** Flow rate as a function of horizontal distance from the nozzle of the Suppression System 1.

### 3.3.1. Suppression System 1

The water suppression System 1 consists of control valves and two open nozzles for each. The control valve sprays water downwards. The two nozzles are located in the middle of the corridor, at height of 2.3 m from the floor spraying towards the cable trays. The control valve is slow (RTI around 150 $(ms)^{1/2}$) and the nominal activation temperature is 68 °C. The nozzles are type Walther LU 25 NW 15 with $K$-value 25 l/min/bar$^{1/2}$.

In the experiment, the nozzle was installed to pendent position at 134 cm height from the floor. The nozzle was spraying water during 7 min in about 5 bar pressure. Result of this experiment is shown in Fig. 5. The total water flow at the same pressure was measured during 30 s to be 27.77 kg which corresponds to flow rate 56 l/min. The spray of this nozzle is not homogeneous and the spray of the model has been also divided into two parts so that the water flow near the nozzle is smaller than farther away. The best fitting model is shown in Fig. 5 and the model parameters are listed in Table 3.

### 3.3.2. Suppression System 2

The suppression System 2 consists of control valves under the ceiling and four open nozzles controlled by one control valve. This control valve does not spray water. The nozzles are fastened to the trays pointing to the trays at the opposite side, at two different heights. The lower pair of nozzles is at height 1.8 m and the upper at 3.5 m from the floor. The pair of nozzles is not exactly towards each other, but they have some 1.7–1.8 m distances in $x$-direction. The control valve is fast (RTI not over 50 $(ms)^{1/2}$) and the nominal activation temperature is 68 °C. The open nozzles are type Tyco D-3 Protectospray 180° No. 32 with $K$-value 80.6 l/min/bar$^{1/2}$.

In the experiment, this nozzle was installed at 1.765 m from the floor. The nozzle was on during 3:05 min with pressure 3.7 bar. The flow rate was measured with the barrel. During 52 s the water accumulation was 152.8 kg which corresponds to flow rate 159 l/min. The flow area of this nozzle is much wider than that of the nozzle in System 1. The best fitting model is shown in Fig. 6 and the model parameters of this nozzle are listed in Table 3.

The effective pressure in the pipes depends on how many sprinklers or nozzles are operating at the moment. The pressure when no sprinklers are operating is 10 bar. The pressure as a function of operating sprinklers is shown in Table 4.

**Table 3**
Model parameters of the nozzles in the suppression systems.

| | Spray angle (°) | Droplet velocity (m/s) | Flow rate at 5 bar | Droplet median diameter (μm) | Offset |
|---|---|---|---|---|---|
| Nozzle (System 1) | 20% 40–50<br>80% 50–75 | 40 | 56 | 700 | 0.1 |
| Control valve (System 1) | 60–80 | 14 | 56 | 700 | 0.1 |
| Nozzle (System 2) | 1% 0–9<br>36% 9–60<br>63% 60–90 | 23 | 160 | 500 | 0.1 |

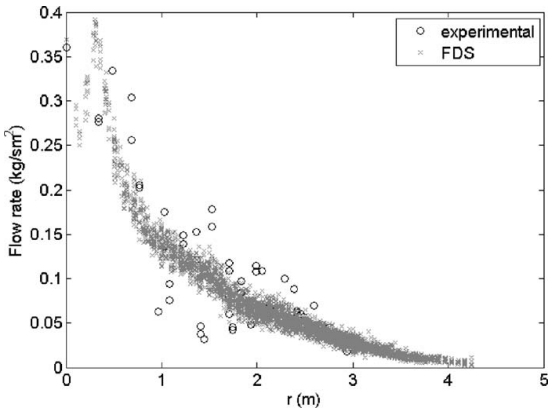


**Fig. 6.** Flow rate as a function of horizontal distance from the nozzle of the Suppression System 2.

### 3.4. Fire detection

In addition to the suppression system, the tunnel is also equipped with OMNI-type fire detectors having three activation criteria: ion, optical and temperature. When any of the criteria is fulfilled, the detector alarms. In the simulations, three separate detectors are placed under the ceiling, to the middle of the length of the first computational mesh. The ion detector is called *smoke* detector in FDS. The FDS implementation is an idealization of a spot-type smoke detector. The change in the mass fraction of smoke in the sensing chamber can be found by solving

$$\frac{dY_c}{dt} = \frac{Y_e(t) - Y_c(t)}{L/u}, \tag{7}$$

where $Y_c$ is the mass fraction of smoke in the sensing chamber, $Y_e$ is the mass fraction in the external free stream, $L$ is length characteristic of the detector geometry and $u$ is the free stream velocity. The detector activates when $Y_c$ rises above the threshold value. The optical smoke detector is called *beam*. The user has to specify the emitter and receiver positions and the total obscuration at which the detector will alarm. FDS integrates the obscuration over the path length using the predicted soot concentration in each grid cell along the path. The temperature in the *heat* detector follows the equation

$$\frac{dT_l}{dt} = \frac{\sqrt{|u|}}{\mathrm{RTI}}(T_g - T_l), \tag{8}$$

where subscript $l$ denotes to link and $g$ to gas. As no information was available of the original detector parameters, the values were estimated by expert judgment and listed in Table 5.

### 3.5. Tenability criteria for human actions

The conditions of the fire environment were monitored inside the tunnel to allow the estimation of the probability of successful fire extinction by fire fighters. Three physical conditions were considered: gas temperature, incident thermal radiation and visibility. The physical conditions were monitored at 7.5–9.25 m horizontal distance from the middle point of the fire source, depending on the location of the source. The conditions at three vertical heights from the floor were monitored: 0.5 m, 1.0 m and 1.5 m.

Since there are no generally accepted values for the tenability limits, rather crude values were here used to give a rough estimation of the time when the possibilities of the fire fighters to find and extinguish the fire are seriously decreased. The tolerable conditions were defined to be (at 0.5–1.5 m from the floor)

- temperature $\leq 100\,^{\circ}\mathrm{C}$,
- visibility $\geq 1$ m,
- radiative heat flux $\leq 10\,\mathrm{kW/m^2}$.

## 4. Probabilistic simulations

The Monte Carlo simulations were performed with two suppression systems and without any. Monte Carlo technique was implemented using Probabilistic Fire Simulator version 4. The random variables and the associated distributions are listed in Table 6. A FDS model was created and input template was added to the user interface of PFS. During the simulation, the FDS input parameters depending on some of the random variables were linked to the realized values of the random variables. The sample size was set in each simulation to 100 LHC samples, and corresponding amount of FDS input files was created by PFS. The simulations were carried out using FDS versions 5.2.4–5.4.3, using parallel processing. After all the simulations were completed, the results were read and post-processed using PFS.

The model had 14 random variables (listed with their distributions in Table 6). The distributions are mostly uniform or triangular as more accurate information was not available. For concrete wall properties several different literature values were available and some of them are listed in Table 7. The parameter ranges were chosen to cover most of the literature values. The thicknesses of the power cable layers vary ±50% of the thicknesses of the NOKIA AHXCMK 10 kV $3 \times 95/70\,\mathrm{mm^2}$ power cable model. The sprinkler properties RTI and $T_a$, and the horizontal distance $x$ are not vari-

**Table 4**
Effective pressure as a function of operating nozzles and sprinklers.

| Number of operating nozzles | Pressure (bar) |
|---|---|
| 1 | 10 |
| 4 | 8 |
| 7 | 6 |

**Table 5**
Parameters used for the OMNI-detector.

| | Quantity | Threshold value | Parameters |
|---|---|---|---|
| Smoke | Chamber obscuration | 3.28%/m | Length = 1.8 m |
| Beam | Path obscuration | 33% | – |
| Heat | Link temperature | 68 °C | RTI = 150 $(\mathrm{ms})^{1/2}$ |

**Table 6**
Random variables and their distributions in the Monte Carlo simulations. Parameters are listed in form of min, max for uniform and peak, min, max for triangular distribution.

| | Distribution | Parameters |
|---|---|---|
| **Burner** | | |
| $x_b$ | Uniform | 0, 1.75 |
| $z_b$ | Discrete | |
| $Q_{max}$ | Triangular | 500, 300, 700 |
| $t_{peak}$ | Triangular | 1200, 900, 1500 |
| **Sprinkler** | | |
| RTI – slow | Triangular | 150, 120, 180 |
| RTI – fast | Triangular | 37.5, 25, 50 |
| $T_a$ | Triangular | 68, 61, 75 |
| **Concrete wall** | | |
| $k$ | Uniform | 1.4, 1.8 |
| $c_p$ | Uniform | 0.6, 1.0 |
| $\rho$ | Uniform | 2100, 2500 |
| **Power cable** | | |
| $k$ (sheath) | Triangular | 0.05, 0.01, 0.3 |
| $d$ (sheath 1) | Uniform | 0.625, 1.875 |
| $d$ (insulation) | Uniform | 3.0, 9.0 |
| $d$ (sheath 2) | Uniform | 1.25, 3.75 |

ables in the simulations without sprinklers. The slow RTI value is used in the simulations with suppression System 1 and the fast with suppression System 2.

The calculation of the droplets is the most computationally expensive part of the simulations. To reduce the calculation time, a stopping condition was created to turn the nozzles off after the fire has certainly died. The stopping condition consists of three criteria, and each of them has to be fulfilled before the condition is taking effect. The criteria are:

- Time is greater than the burner flame-out time.
- The fire heat release rate is less than 1 kW.
- The temperature in the ceiling is less than 25 °C.

The stopping condition was only used in the simulation of suppression System 2.

## 5. Results and discussion

### 5.1. Simulation results

When either of the suppression systems was used, the peak heat release rates (HRRs) during the simulations were reduced to about 10% of the non-sprinklered values. The cumulative probability distributions of the peak HRR are shown in Fig. 7. The highest peak HRR without sprinklers was more than 60 MW while with suppression System 1 it was around 5 MW and with suppression System 2 less than 4 MW.

The most significant correlation coefficients between the peak HRR and the random variables are listed in Table 8. The most significant variable to peak HRR was in all the simulations the $z$-coordinate of the ignition point. It deserves consideration that without a suppression system and with System 1, the correlation was negative, meaning that higher ignition point leads to smaller fire. This is probably due to the reduced amount of combustible cables above the burner that could be easily heated up and ignited.

**Table 7**
Some literature values for concrete properties.

| | Harmathy (1995) | Iwankiw et al. (2004) |
|---|---|---|
| $\rho$ (kg/m$^3$) | 2150–2450 | 2323 |
| $k$ (W/m K) | 1.37, 1.4–2.5 | 1.64 |
| $c_p$ (W/m K) | 0.88, 0.6–0.85 | 0.84 |

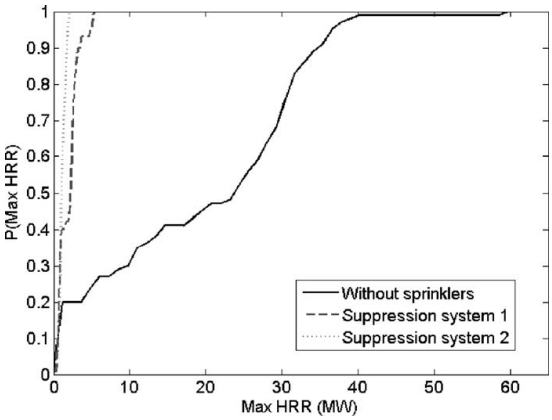


**Fig. 7.** Comparison of the cumulative probability distributions of the peak heat release rate.

With System 2, the correlation was positive. The reason lies in the placement of the upper open nozzles: System 2 does not have any nozzle just below the ceiling as System 1, but there is an extra pair of nozzles at the height 3.5 m protecting the lower power cable trays from igniting. However, they cannot protect the cable trays close to the ceiling from igniting. The peak HRR with System 2 is not sensitive to other variables, but in the other simulations the specific heat capacity of concrete wall and the peak HRR of the initial burner are also significant. The simulations with System 1 are also sensitive to the thickness of the first sheath layer and the density of concrete wall.

Without sprinklers, all the power cables and 60% of the IC cables passed both failure limits (180 °C and 220 °C). The power cable failures occurred in the time frame 700–1500 s and IC cable failures in the time frame 1000–1800 s. With suppression systems, no failures occurred. The peak power cable temperatures were 120 °C in case of System 1 and 170 °C in case of System 2. IC cables remained far below the failure temperatures with both suppression systems, the maximum being 50–60 °C. The cumulative probability distributions of the peak cable temperatures at the insulation layer are shown in Fig. 8. The high temperatures in the case with no suppression system correspond to conditions where the cables would be burning, and the temperature is controlled by the local flame heat transfer, not global conditions affected by the random boundary conditions. System 2 protects the IC cables slightly better than System 1. However, the power cables are much better protected with System 1. This confirms that the upper nozzles at this position are not necessarily enough for protecting the ceiling.

The significant correlations for the cable temperatures are listed in Table 9. The power cable correlations in the non-sprinkled case are not given, due to the above mentioned reason. The most significant parameters are the $z$-coordinate of the ignition point, concrete wall's specific heat capacity and the thickness of the first

**Table 8**
Significant correlations between the peak HRR and random variables. Confidence level ≥0.95 to be unequal to zero.

| | No suppression | System 1 | System 2 |
|---|---|---|---|
| $z_b$ | −0.86 | −0.85 | 0.30 |
| $c_p$ (concrete) | −0.21 | 0.20 | – |
| $Q_{max}$ | 0.24 | 0.24 | – |
| $\rho$ (concrete) | – | −0.21 | – |
| $d$ (sheath 1) | – | −0.29 | −0.20 |
| $x$ | – | – | −0.29 |

**Table 9**
Significant correlations with the maximum temperature of the cables with confidence level ≥0.95.

| | IC cable | | | Power cable | |
|---|---|---|---|---|---|
| Parameter | No suppression | System 1 | System 2 | System 1 | System 2 |
| $z_b$ | −0.93 | −0.97 | −0.66 | −0.91 | 0.65 |
| $c_p$ (concrete) | −0.22 | 0.24 | – | – | – |
| $Q_{max}$ | 0.21 | – | – | – | – |
| $d$ (sheath 1) | – | – | – | −0.40 | – |
| $d$ (insulation and filler) | – | – | 0.30 | – | – |

sheath layer. In the light of the correlation coefficients, the peak temperatures behave in a similar manner as the peak HRR: high ignition point causes smaller temperatures, except for System 2, where the fires became more severe and the power temperatures higher. Interestingly, the high ignition point does not cause higher temperatures for the IC cables protected by System 2.

In most of the cases all four sprinkler units activated. The cumulative probability distributions of both suppression systems are shown in Fig. 9. With System 2, the probability of only one or two activated units is a bit higher than with the System 1. The significant correlations are listed in Table 10. Both systems are sensitive to the ignition point $z$-coordinate. System 1 is also negatively correlated with the $x$-coordinate of the ignition point and the concrete specific heat capacity. System 2 is correlated with RTI of the control valve and the peak HRR of the initial burner.

In the simulations without sprinklers, only the temperature criteria were met (2–49% probability depending on the altitude). On

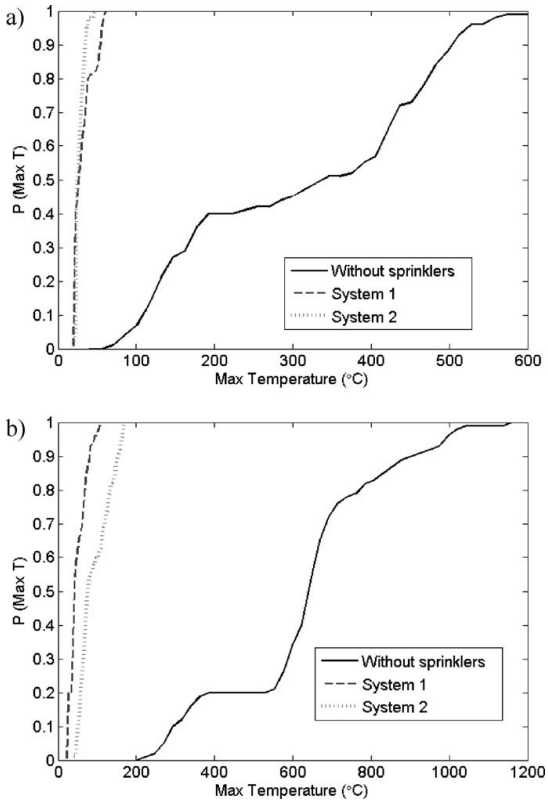


**Fig. 8.** The cumulative probability distributions of the peak internal cable temperatures. (a) IC cables. (b) Power cables.

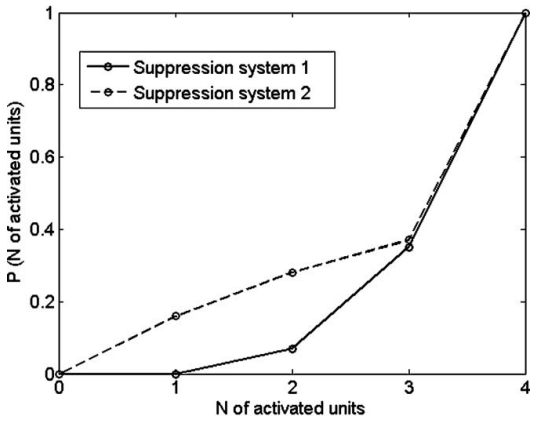


**Fig. 9.** Cumulative probability distributions for number of activated suppression units (control unit and nozzles).

**Table 10**
Significant correlations between the number of activated sprinklers and random variables with confidence ≥0.95 of not being zero.

| | System 1 | System 2 |
|---|---|---|
| $z_b$ | −0.74 | – |
| $x_b$ | −0.24 | – |
| $c_p$ (concrete) | −0.21 | – |
| $Q_{max}$ | – | 0.19 |

the other hand, in the simulations with any suppression system, the only condition to exceed the limits was the visibility, which was lost in all cases. The cumulative distributions for the time when the tenability criteria were met are shown in Fig. 10. The visibility is lost fastest (between 12 and 25 min from the beginning) in the simulations with System 2. With System 1 the visibility is lost a bit later, between 16 and 30 min from the beginning. Without suppression systems, the temperature exceeds 100 °C in less than 50% of the simulations. If it happens, it happens after 20 min from the beginning. These times are in the same range with the cable failure times, meaning that if the fire brigade can reach the fire compartment before the failures, they also have good possibilities to actually reach actual fire location. The poor visibility in case of activated sprinklers will make finding the fire source very difficult.

The cable failures may be prevented if the fire is detected early and the fire brigade has time to operate. The details about the OMNI detector used for detecting the fire is described in Section 3.4. The detector activates when any of the three criteria (heat, ion or optical) exceeds the critical value. The activation times of the fire detectors are shown in Fig. 11. The ion and optical detectors were always the first ones to go off – the heat detector was much slower and did not always reach the critical value when sprinklers were used. For the case without water suppression, the ion detector was always slightly faster than the optical detector, with mean difference of 13 s. The ion detector was faster than optical in 64%

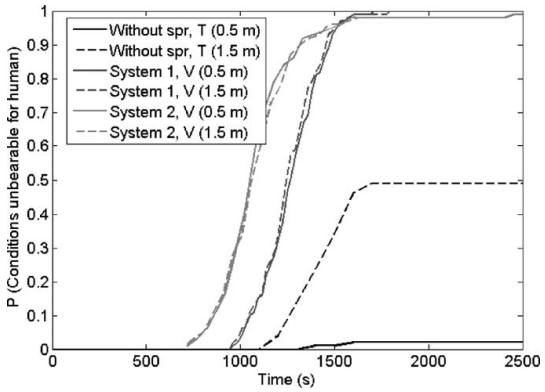


**Fig. 10.** Cumulative probability distributions for the time that the conditions for human get intolerable 7.5 m away from the ignition point. T, temperature criterion; V, visibility criterion.

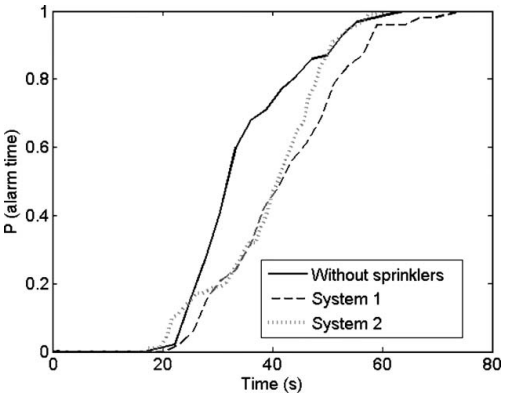


**Fig. 11.** Cumulative probability distributions of smoke alarm activation times.

of the cases when suppression System 1 was used, and in only 8% with suppression System 2. The mean delays were the same order of magnitude as for the non-suppressed case. These results are in line with the results of Fig. 10, where the visibility is lost much faster with suppression System 2 than with System 1. Soot yield is assumed to be 5% in the simulations. At the time of the OMNI detector activations, none of the sprinklers has been activated and all the systems are similar in this sense. The only difference comes from the $x$-location of the burner which is constant in the simulations without sprinklers. The small differences in the cumulative distributions are caused by the different random variables. The alarm activates between 20 and 80 s from the ignition of the fire. The heat release rates at the time of the alarms are less than 10 kW.

### 5.2. Sensitivity study

The random variables of the Monte Carlo simulation covered the uncertainty associated with the unknown location and properties of the initial fire, properties of the sprinkler heads and surrounding walls and the variability in the power cables. The simulations were performed using the existing (System 1) or proposed (System 2) design values of the sprinkler system. Additional simulations were performed to study the sensitivity of the simulation outcome on

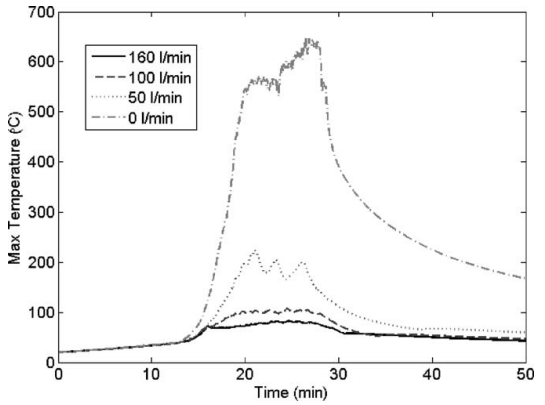


**Fig. 12.** The maximum power cable temperatures at different flow rates of the nozzles.

the two of the sprinkler system design values: water flow rate and installation height.

The flow rate of the nozzles depends strongly on the pressure in the pipes. If the pressure drops due to some fault or because too many nozzles are operating at the same time, the suppression system may not be able to protect the room as designed. The same simulation of the suppression System 2 was repeated with flow rates varying between 0 and 160 l/min. As long as the flow rate was at least 50 l/min, it was found to have no significant effect on the heat release rate or the peak temperature of the IC cables, but the difference between 50 l/min and 0 l/min is remarkable. The effect of the flow rates is seen best from the peak temperature of the power cables (Fig. 12). The nozzles with flow rate of 50 l/min or less are not able to protect the power cables from exceeding the failure temperature in this case.

Above, it was suspected that the efficiency of the suppression System 2 may be sensitive to the height of the upper nozzles. The same simulation was repeated varying the height of the upper nozzles. The results are shown in Figs. 13 and 14. However, the differences were not significant and the temperatures remained well below the failure limit in all cases.

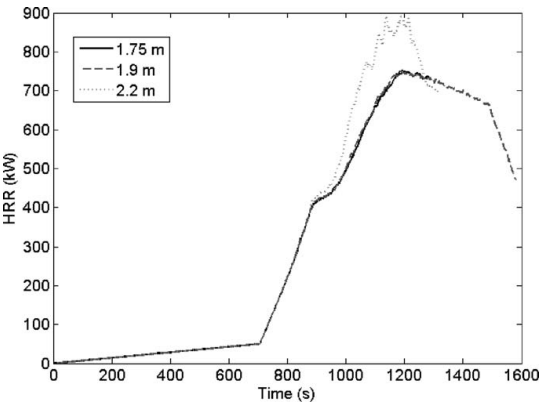


**Fig. 13.** Heat release rate in the simulation with different upper nozzle heights. The legend indicates the distances from ceiling.

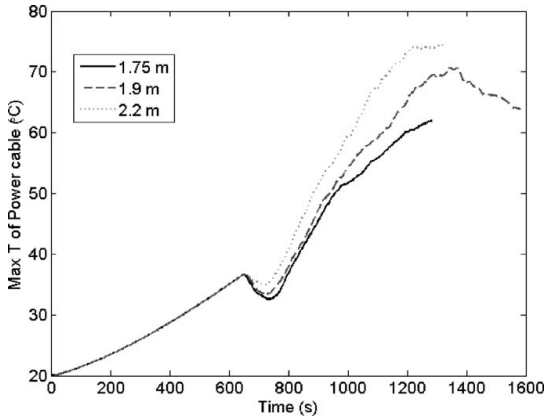


**Fig. 14.** The maximum temperature of the power cables with different upper nozzle distances from the ceiling. The legend indicates the distances from ceiling.

## 6. Conclusions

Cable fires inside a cable tunnel of a nuclear power plant were simulated using Monte Carlo technique and FDS code as a deterministic tool. The fire development on the power cables was predicted using a pyrolysis model, and the performance of the water based suppression systems was simulated using physical modelling of the sprinkler activation and two-phase flows. Three separate MC simulations were performed with 100 LHC samples for each, to find out the differences between two water suppression systems and the case without any suppression system. Some of the model parameters associated with the placement of the ignition point, tunnel properties and cable properties, were treated as random variables with probability distributions. The results included the probability distributions of the peak heat release rate in the room, cable failure times, alarm times and the conditions for a fire fighter entering the room.

In the case without fire suppression, the predicted peak heat release rates varied between 2 and 60 MW. When suppression was used, the peak HRRs were generally less than 10% of the ones without suppression. The suppression effect on the cable failures was clear as well. Without suppression, almost all power cables and 60% of the IC cables of the second sub-system failed due to the thermal damage, but failures did not occur when either of the two suppression system was used. From the viewpoint of the plant PRA, this is an extremely interesting result because it means that that the probability of losing both sub-systems is determined by the unavailability of the suppression system.

The temperature of the cables in the second sub-system was mostly dependent on the height of the ignition point, but the direction of the effect was dependent on the suppression system. The internal temperatures of the power cables were higher with suppression System 2. According to the current results, the performance of a suppression system similar to System 2 may be very sensitive to the actual distance of the upper nozzles from the ceiling. As the system has no ceiling nozzle, it cannot prevent fire spread and failures in the highest cable trays if the upper nozzles are designed to be placed too low.

In most simulations, the conditions would remain tolerable for a fire fighter reaching the fire before cable failures. In the simulations without suppression system, the temperature exceeded 100 °C with a 50% probability. In the simulations with suppression system, the heat was not a problem but the visibility was lost in all the cases. The smoke alarms were activated quite early in all fires, between 20 and 80 s from the ignition.

Overall, the current results concerning the efficiency of the sprinkler systems should be considered conservative because the power of the ignition source is not affected by the sprinkler activation. In reality, the ignition source already could be suppressed by the sprinklers. This finding indicates that the accurate simulation of fire development from its early phases is extremely important for the completeness and accuracy of the probabilistic, simulation based fire risk assessment. Despite the many advances in our capability to simulate fire spreading and fire dynamics, the focus of the fire research should remain in this topic, as it is still far from solved.

Another topic where more research and, in particular, full scale validation of the models is needed, is the simulation of water suppression. Both the physical and numerical simulation problems observed during this work indicate that the models of the two-phase flows and suppression effects are far from mature. The importance of the water suppression system was evident because the PVC cables burn easily and impose a high fire risk. They are still widely used in the nuclear installations around the world, but in the new or renovated installations, the fire performance of the electrical cables may be significantly better due to the use of flame retardant materials. The safety importance of the suppression system may be much smaller in such cases, but the risks in these situations have not been generally evaluated.

## Acknowledgements

We thank Dr. Tuula Leskelä of Aalto University, for performing the thermoanalytical experiments. We also thank Dr. Johan Mangs and Mr. Konsta Taimisalo from VTT for the cone calorimeter experiments. This work was funded by the State Nuclear Waste Management Fund (VYR).

## References

Andersson, P., Van Hees, P.,2005. Performance of cables subjected to elevated temperatures, fire safety science. In: Proceedings of the Eighth International Symposium. International Association for Fire Safety Science, pp. 1121–1132, doi:10.3801/IAFSS.FSS.8-1121.

Chien, S.-W., Huang, Y.-H., Shen, T.-S., Lin, C.-Y., Cheng, T.-M., 2006. How does a sprinkler system perform in a nuclear power plant? Journal of Applied Fire Science 15 (3), 201–217, doi:10.2190/AF.15.3.c.

Dreisbach, J., McGrattan, K., 2008. Cable Response to Live Fire (CAROLFIRE) Volume 3: Thermally-Induced Electrical Failure (THIEF) Model., NUREG/CR-6931, Vol. 3 NISTIR 7472.

Dreisbach, J., Hostikka, S., Nowlen, S.P., McGrattan, K., 2010. Electrical cable failure – experiments and simulation. In: 12th International Interflam Conference, pp. 1857–1865.

Ferng, Y.M., Liu, C.H., 2011. Investigating the burning characteristics of electric cables used in the nuclear power plant by way of 3-D transient FDS code. Nuclear Engineering and Design 41, 88–94, doi:10.1016/j.nucengdes.2010.08.021.

Harmathy, T.Z., 1995. Properties of building materials. In: The SFPE Handbook of Fire Protection Engineering, 2nd edition, Section 1, Chapter 10 and Appendix B (table B-7).

Hostikka, S., Keski-Rahkonen, O., 2003. Probabilistic simulation of fire scenarios. Nuclear Engineering and Design 224, 301–311.

Hostikka, S., 2008. Development of fire simulation models for radiative heat transfer and probabilistic risk assessment. VTT publications 683, Doctoral dissertation.

Iwankiw, N., Beitel, J., Gewain, R., 2004. Structural materials. In: Harper, C. (Ed.), Handbook of Building Materials for Fire Protection. McGraw-Hill Handbooks, New York.

Mangs, J., Keski-Rahkonen, O., 1997. Fullscale fire experiments on vertical and horizontal cable trays. VTT publications 324, Espoo, 58 pp. + app. 44 pp.

Matala, A., Hostikka, S., Mangs, J.,2008. Estimation of pyrolysis model parameters for solid materials using thermogravimetric data. In: Fire Safety Science – Proceedings of the Ninth International Symposium. International Association for Fire Safety Science, pp. 1213–1223.

McGrattan, K., Hostikka, S., Floyd, J., Baum, H., Rehm, R., Mell, W., McDermott, R., 2007. Fire Dynamics Simulator (Version 5), Technical Reference Guide. Volume 1: Mathematical Model. National Institute of Standards and Technology, Gaithersbug, MD, NIST Special Publication 1018-5.

McGrattan, K., McDermott, R., Hostikka, S., Floyd, J., 2010. Fire Dynamics Simulator (Version 5) User's Guide. National Institute of Standards and Technology, Gaithersburg, MD, NIST Special Publication 1019-5.

McKay, M., Beckman, R., Conover, W., 1979. A comparison of three methods for selecting values of input variables in the analysis of output from a computer code. Technometrics 21 (2), 239–245.
Paté-Cronell, M.E., Dillon, R.L., 2006. The respective roles of risk and decision analyses in decision support. Decision Analysis 3 (4), 220–232.
Shen, T-S., 2006. Will the second cable tray be ignited in a nuclear power plant? Journal of Fire Sciences 24, 265–274.
Stein, M., 1987. Large sample properties of simulations using Latin Hypercube sampling. Technometrics 29 (2), 143–151.
U.S. NRC, 2005. EPRI/NRC-RES Fire PRA Methodology for Nuclear Power Facilities: Volume 2: Detailed Methodology. Electric Power Research Institute (EPRI)/U.S. Nuclear Regulatory Commission, Office of Nuclear Regulatory Research (RES), Palo Alto, CA/Rockville, MD, EPRI – 1011989 and NUREG/CR-6850.